

Adaptive Variational Quantum Kolmogorov-Arnold Network

Hikaru Wakaura^{1,*}, Rahmat Mulyawan^{2,3,/}, and Andriyan B. Suksmono^{2,3,4,+}

¹QuantScape Inc. QuantScape Inc., 4-11-18, Manshon-Shimizudai, Meguro, Tokyo, 153-0064, Japan

²The School of Electrical Engineering and Informatics, Institut Teknologi Bandung (STEI-ITB), Jl. Ganesha No.10, Bandung, Indonesia

³Research Collaboration Center for Quantum Technology 2.0, BRIN-ITB-TelU, Indonesia

⁴ITB Research Center on ICT (PPTIK-ITB)

*hikaruwakaura@gmail.com

/rahmat.mulyawan@itb.ac.id

+suksmono@itb.ac.id

ABSTRACT

Kolmogorov-Arnold Network (KAN) is a novel multi-layer neuromorphic network. Many groups worldwide have studied this network, including image processing, time series analysis, solving physical problems, and practical applications such as medical use. Therefore, we propose an Adaptive Variational Quantum Kolmogorov-Arnold Network (VQKAN) that takes advantage of KAN for Variational Quantum Algorithms in an adaptive manner. The Adaptive VQKAN is VQKAN that uses adaptive ansatz as the ansatz and repeat VQKAN growing the ansatz just like Adaptive Variational Quantum Eigensolver (VQE). The scheme inspired by Adaptive VQE is promised to ascend the accuracy of VQKAN to practical value. As a result, Adaptive VQKAN has been revealed to calculate the fitting problem more accurately and faster than Quantum Neural Networks by far less number of parametric gates.

1 Introduction

The rapid progress in artificial intelligence (AI) has been primarily fueled by neural network models inspired by the architecture of the human brain¹. These models, built on interconnected artificial neurons or perceptrons^{2,3}, have achieved outstanding success in applications ranging from image recognition to natural language processing⁴. However, traditional neural networks encounter significant scalability and computational efficiency challenges when dealing with large-scale data, posing a bottleneck to further advancements in AI. To address these challenges, researchers have been investigating alternative network architectures. One such promising approach is the Kolmogorov-Arnold Network (KAN), recently introduced by Tegmark's group⁵. KAN enhances computational efficiency by optimizing synaptic weights through direct manipulation of neuron parameters, leveraging matrix operations for streamlined computation. Moreover, this innovative design allows the network to be interpreted and implemented as a quantum circuit, paving the way for seamless integration of quantum computing into neural network frameworks. As a result, many groups worldwide began researching the theory and application of KAN. Though there are some critical opinions⁶, there are already a lot of research reported for example image analysis⁷, time-dependent analysis⁸, and solving problems in physics^{9,10}. KAN is good at solving. Furthermore, it is applied for controlling spacecraft and medical use^{11,12}.

In this context, we propose an Adaptive Variational Quantum Kolmogorov-Arnold Network (VQKAN). VQKAN¹³ is KAN on a variational quantum framework for quantum machine learning that uses measurement results of qubits as neurons and quantum gates as synapses. The framework of VQKAN is the same as Variational Quantum Algorithms (VQAs). The VQKAN utilizes the multi-layer architecture, parametric gates, and feedback to reproduce the KAN scheme by modifying the Variational Quantum Eigensolver (VQE) scheme. Quantum computing algorithms, particularly Variational Quantum Algorithms (VQAs), have experienced remarkable advancements in recent years. Foundational contributions from Aspuru-Guzik and collaborators¹⁴ have paved the way for algorithms such as the Variational Quantum Eigensolver (VQE)¹⁵, Adaptive VQE¹⁶, and Multiscale Contracted VQE (MCVQE)¹⁷. These algorithms are highly compatible with Noisy Intermediate-Scale Quantum (NISQ) devices and have found applications in quantum machine learning tasks¹⁸⁻²⁶. This integration of quantum computing with AI demonstrates the transformative potential of quantum approaches in enhancing the performance and efficiency of artificial intelligence models. The VQKAN is more robust for overfitting than the Quantum Neural Network (QNN)²⁷. However, prediction accuracy is low for practical use; thus, the optimization method, ansatz, and method itself must be modified to

improve accuracy. Therefore, we propose Adaptive VQKAN, which optimizes the parameters and state by repeating VQKAN with adaptive ansatz growing it. The Adaptive VQE is one of the most accurate methods for calculating the energies of molecules. Thus, adaptive ansatz and the manner of Adaptive VQE are promised to be more accurate than ordinary VQKAN.

We perform optimization on fitting, classification problems, and solving Fourier differential equations using Adaptive VQKAN. As a result, Adaptive VQKAN is revealed that it is unable to optimize on the classification problem, able to optimize on the fitting problem more accurately and faster than QNN, and able to optimize on solving Fourier differential equation less accurately and faster than QNN. Besides, the number of parametric gates is far smaller than that of QNN. This method is also expected to require far less number of parameters to calculate as accurate as Quantum KAN²⁸.

Section 1 is the introduction, section 2 describes the method detail of Adaptive VQKAN and the optimization method, section 3 describes the result on fitting, classification problem, and solving Fourier differential equation, Section 4 is the discussion of results, and section 5 is the concluding remark.

2 Method

In this section, we introduce the Adaptive Variational Quantum Kolmogorov-Arnold Network (VQKAN) method.

VQKAN is the variational quantum algorithm version of KAN, a multi-layer network based on the connection of synapses in neurons.

First, initial state $|\Psi_{ini}(\mathbf{1}\mathbf{x}^m)\rangle$ is $\prod_{j=0}^{N_q-1} Ry^j(2acos(\sqrt{1\mathbf{x}_j^m})) |0\rangle^{\otimes N_q}$ for each input m . $Ry^j(\theta)$ is θ degrees angle rotation gate for y-axis on qubit j . $n\mathbf{x}^m$ is the input vector at layer n for m -th input data. We will describe later that the Loss function is calculated similarly to Subspace-search VQE²⁹, and multiple points are calculated at once.

For Adaptive VQKAN, $\phi_{jk}^{np}(n\mathbf{x}^m)$ is the gate of the angle.

$$\phi_{jk}^{np}(n\mathbf{x}^m) = \sum_{i \in \{0, dim(n\mathbf{x}^m)\}}^{N_d^n - 1} 2acos(E_f(n\mathbf{x}_i^m) + \sum_{s=0}^{N_g - 1} \sum_{l=0}^{N_s - 1} c_s^{npjkl} B_l(n\mathbf{x}_i^m)) \quad (1)$$

, which N_d^n is the number of input for layer n , N_g is the number of grids foreach gate, N_s is the number of splines, respectively.

Then, c_s^{npjkl} and $B_l(n\mathbf{x}_i^m)$ are the parameters to be trained, initialized into 0 and spline functions at layer n , respectively, the same as classical KAN. $n\mathbf{x}^m$ is the input vector at layer n , j and k are the index of qubits, respectively. $E_f(n\mathbf{x}_i^m) = x_i^m / (\exp(-n\mathbf{x}_i^m) + 1)$ is the Fermi-Dirac expectation energy-like value of the distribution. The component of $n\mathbf{x}$ is the expectation value of the given observable for the calculated states of qubits. The layer corresponds to the quantum circuit to make a superposition state called ansatz. In this paper, the ansatz is adaptive ansatz, which is the time propagator for selected operators.

$$\Phi_n^A = M \prod_{p=0}^{N_p^n - 1} \exp(iP_p(j, k)\phi_{jk}^{np}(n\mathbf{x}^m)). \quad (2)$$

Then, $P_p(j, k)$ is the p -th operator on j and k -th qubits, and N_p^n is the Number of operators on the n -th layer, respectively. The quantum circuit depicted in Fig. 1 can implement the time propagator. For example, time propagator for $\theta X_1 Y_3 Z_4$ can be implemented by substituting G_1 and G_1^\dagger into H gate, G_3 into $Rx(\pi/2)$, G_3^\dagger into $Rx(-\pi/2)$, and G_4 and G_4^\dagger into I gate, respectively.

The final state of Adaptive VQKAN is,

$$|\Psi(\mathbf{1}\mathbf{x}^m)\rangle = \prod_{n=1}^{num. of layers N_l} \Phi_n^A M |\Psi_{ini}(\mathbf{1}\mathbf{x}^m)\rangle. \quad (3)$$

The result is readout as a form of the Hamiltonian expectation value H , and the loss function is calculated as follows,

$$l_m = |\langle \Psi(\mathbf{1}\mathbf{x}^m) | H | \Psi(\mathbf{1}\mathbf{x}^m) \rangle - f^{aim}(\mathbf{1}\mathbf{x}^m)| \quad (4)$$

$$L = \sum_{m=0}^{num. of samples N-1} a_m l_m \quad (5)$$

where $f^{aim}(\mathbf{1}\mathbf{x}^m)$ is the aimed value of sampled point m and l_m is the loss function (absolute distance) of point m , respectively. Hamiltonian takes the form $H = \sum_{j=0}^{N_o-1} \theta_j P_j$ for the product of the Pauli matrix P_j , consisting of the Pauli matrix X_j, Y_j, Z_j . N_o is the number of P_j in Hamiltonian.

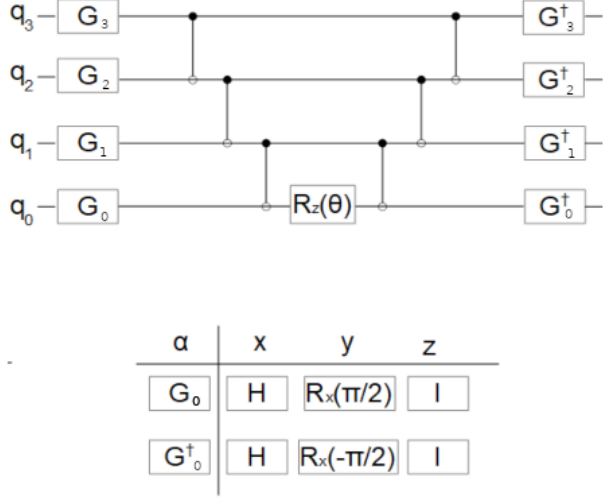


Figure 1. The quantum circuit that perform $\exp(-i\theta\sigma_0^\alpha\sigma_1^\beta\sigma_2^\gamma\sigma_3^\delta)$. G_j gate is H , $R_x(\pi/2)$ or I gate depend on what pauli gate is operated for q_j .

Adaptive VQKAN optimizes the values of the loss function, and the states constructing the adaptive ansatz correspond to the result of VQKAN. In detail, Adaptive VQKAN is performed at first by the initial adaptive ansatz, choosing the new term for ansatz by a given procedure and adding it to the ansatz, and repeating the VQKAN process, with the parameters and N_g the same as at the end of the previous VQKAN process, until the condition for convergence is satisfied. The procedure to choose the new term is two ways: 1. choose the term from the term pool that has the most significant absolute value of gradient in case the term is included at the end of ansatz 2. choose the term from the term pool that have the most minor loss function in case the term is included at the end of ansatz³⁰. The parameter for the new term is 0 for all c_s^{npjk} s, and no new term is added in case the value of the loss function is decreased by adding no terms in the term pool for case 2. If the loss function becomes 10^{-16} or below, the Adaptive VQKAN process converges. We assume $N = 10, a_m = (N - m)/N, N_l = 3, N_q = 4, N_g = 8$ and $N_s = 4(tr + 2)$ for the number of trials tr , respectively. We use blueqat SDK³¹ for numerical simulation of quantum calculations and COBYLA of scipy to optimize parameters but to declare the use of others. We assume that the Number of shots is infinite. All calculations are performed in Jupyter notebook with Anaconda 3.9.12 and Intel Core i7-9750H.

3 Result

In this section, we show the result of Adaptive VQKAN on fitting, classification, and solving Fourier differential equation. The operator pool consists of all combinations of one body Pauli matrices X, Y, Z and two body Pauli matrices XX, XY, XZ, YY, YZ, ZZ and the Number of trials is 1000, and the Number of epochs is 25, respectively.

3.1 Fitting problem

First, we describe the result of the fitting problem. We performed the Adaptive VQKAN on a fitting problem of the following equation on 10 sampled points and predicted the values of 50 test points. The target function is defined as:

$$f^{\text{aim}}(\mathbf{x}) = \exp(\sin(x_0^2 + x_1^2) + \sin(x_2^2 + x_3^2)). \quad (6)$$

Here, $x_i = 2\mathbf{x}_i^m - 1$ for $i = 0, 1, 2, 3$. ${}_n\mathbf{x}_i^m = 0.5(\langle \tilde{\Psi}(\mathbf{x}^m) | Z_i | \tilde{\Psi}(\mathbf{x}^m) \rangle + 1)$ for the state calculated by n-th layer $|\tilde{\Psi}(\mathbf{x}^m)\rangle$, with $N_d^n = 4$ and $\dim({}_n\mathbf{x}^m) = 4$ for all layers and calculations, and the Hamiltonian is $Z_0Z_1 + Z_2Z_3$. The realm of ${}_n\mathbf{x}^m$ is $\{0, 0.25\}$.

The Number of layers $N_l = 1$ and initial ansatz is X_0 , respectively. In advance, we show the result for QNN. The QNN ansatz consists of three layers, as shown in Fig. 2, with a total of 24 parameters initialized randomly. The initial state is $|0\rangle^{\otimes N_q}$.

Fig. 4 (left) displays the loss function for attempt 9, while Fig. 4 (right) presents the fitting results on the test points. Fig. 3 shows the convergence of the loss function over the Number of trials for 10 attempts. The accuracy of prediction is not bad, and the sum of absolute distances is 14.9787 on average.

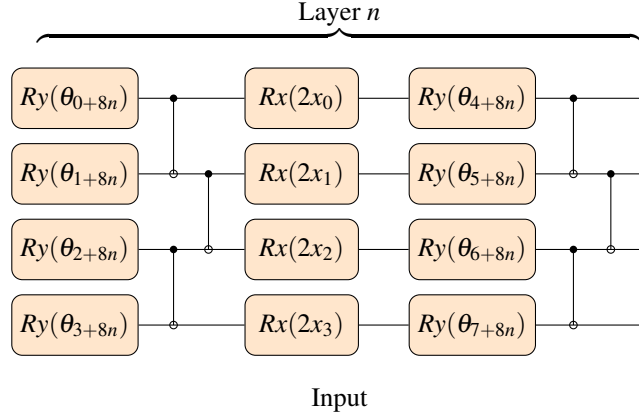


Figure 2. Ansatz structure of the Quantum Neural Network (QNN) with parameterized rotation gates controlled by trainable parameters θ_j . Inputs x_i encode classical data into the quantum circuit, enabling learning through optimization of θ_j to minimize the cost function.

We show the value of the loss function, the sum of absolute distance on test points for the Number of epochs, and absolute distances on test points in Figs. 5 (a)(left), 5 (a)(right), 6(a), respectively for the way 1. The value of the loss function and absolute distances on test points are both more significant than those of QNN, and the absolute distances for test points unstably fluctuate for the Number of epochs. The gradient is supposed not to be effective for searching global minimum because not all of the operators in the operator pool are not complex conjugate.

We show the value of the loss function, the sum of absolute distance on test points for the Number of epochs, and absolute distances on test points in Figs. 5 (b)(left), 5 (b)(right), 6(b), respectively for the way 2. Even though the ansatz is only a single layer, the value of the loss function and the sum of absolute distance are both smaller than those of QNN because the minimum sum for the attempt is 12.7381. The absolute distance for test points is also nearly zero on average, and only a few points are significant. Way 2 is more effective for making optimum adaptive ansatz than way 1. The adaptive ansatz on both ways mainly consists of two-body terms on neighboring qubits.

Next, we show the average of 10 attempts for the value of the loss function and the sum of absolute distance on test points for the Number of epochs of eq. 6, exponential function $\exp((x_1 - x_2)^2/2x_0)$, logarithmic function $\log(x_0/x_1)$, fractional function $1/(1 + x_0x_1)$, radius of sphere which center is zero point in Figs. 7 and 8, respectively in case the Number of epochs is 15 for the way 2. x_i s are the same as eq. 6 except only x_0 for exponential function is $1 - 2_1 \mathbf{x}_0^m$. The value of the loss function and the sum of absolute distance of eq. 6 are both smaller than in all other cases. The Adaptive VQKAN is the most accurate for the fitting problem on above equations except eq. 6 in QNN, VQKAN and Adaptive VQKAN¹³, and the radius of sphere and the required Number of variables is smaller than QNN and VQKAN.

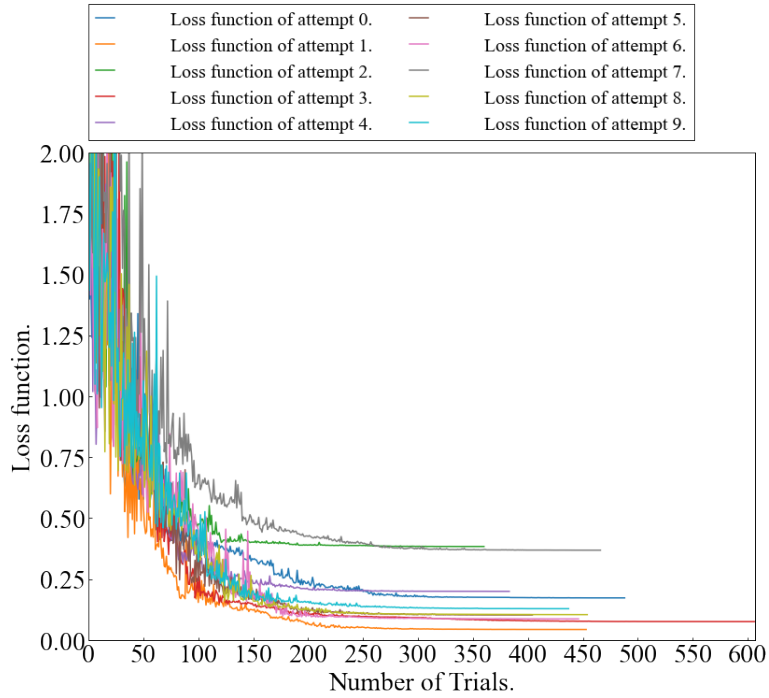


Figure 3. Number of trials vs. loss functions for optimization attempts by QNN.

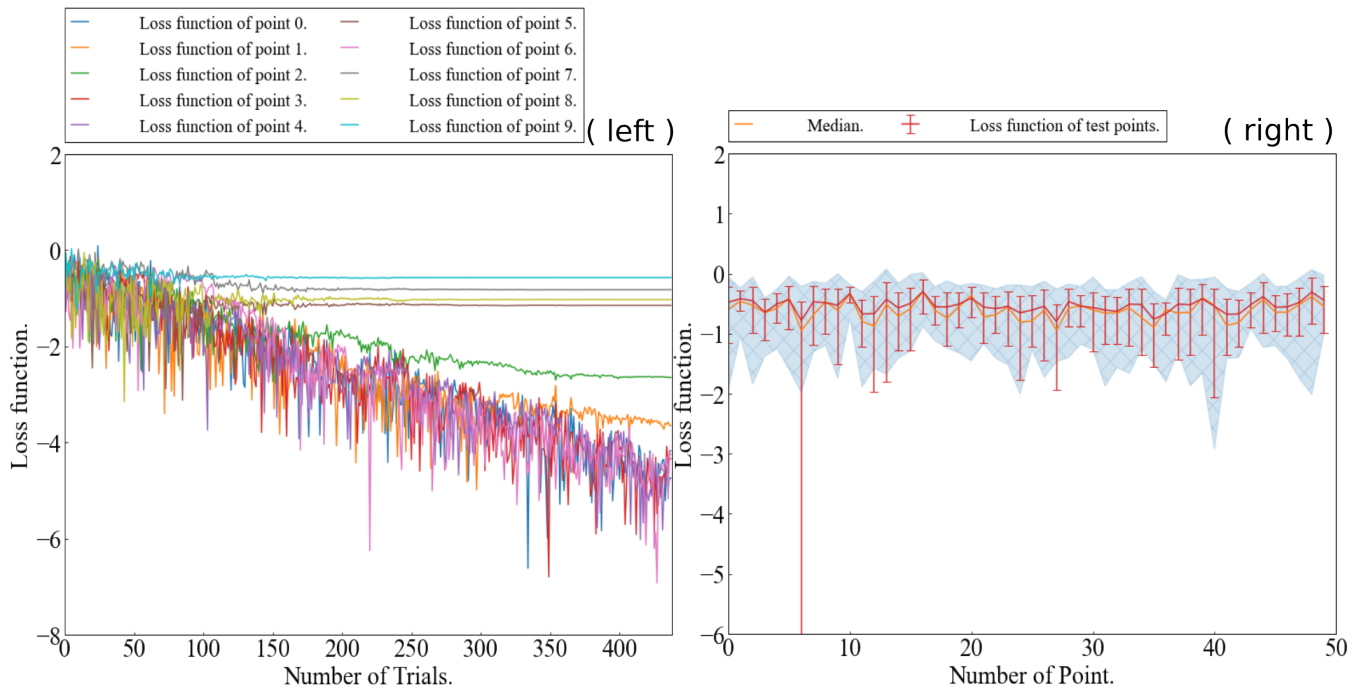


Figure 4. (left) Number of trials vs. loss function in log₁₀ scale for attempt 9 on QNN optimization. (right) Number of test points vs. average and median of absolute distances in log₁₀ scale of test points on QNN optimization. The error bars indicate the standard deviations from the average.

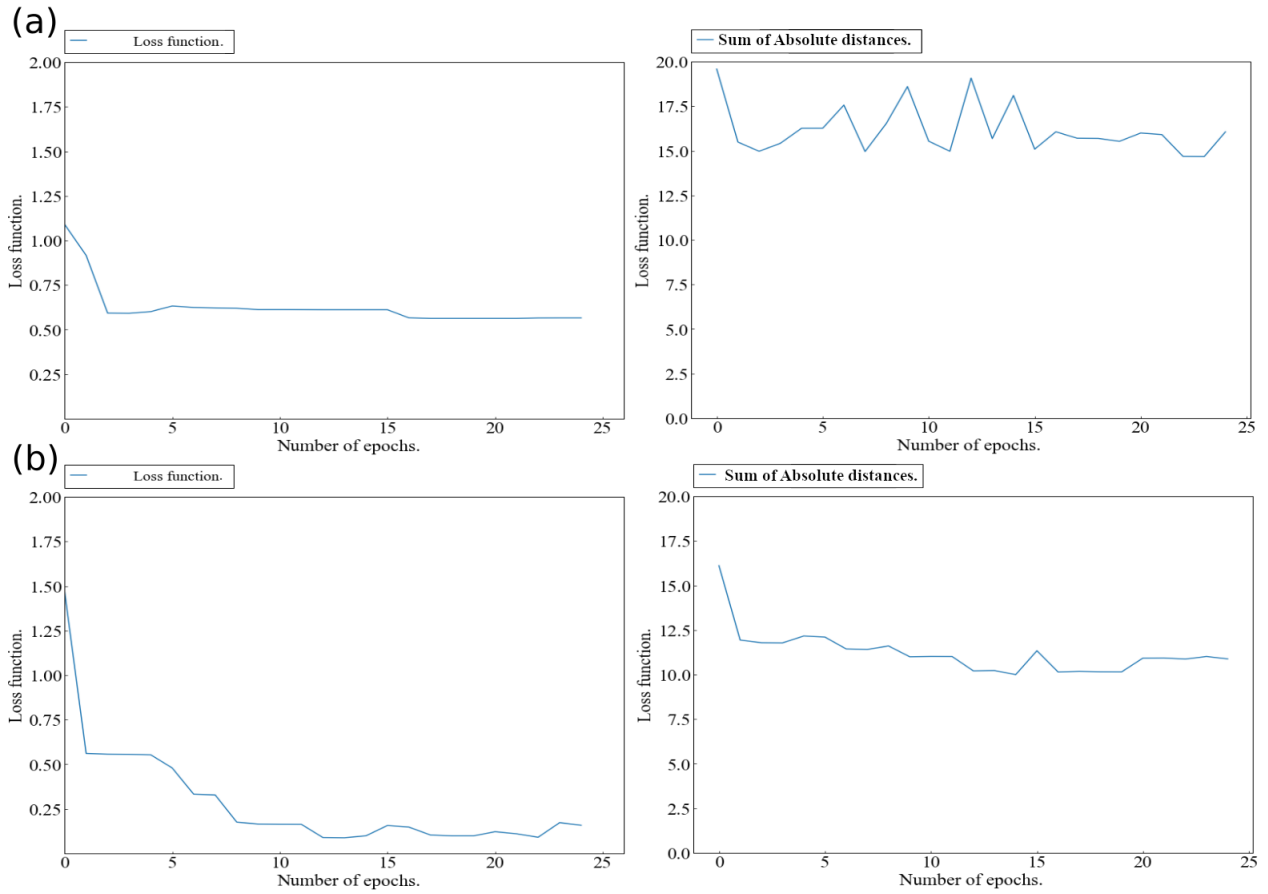


Figure 5. (a)(left) Number of epochs vs. loss functions for optimization attempts on the fitting problem by Adaptive VQKAN for the way 1. (a)(right) Number of epochs vs. sum of absolute distances on the fitting problem by Adaptive VQKAN for the way 1. (b)(left) Number of epochs vs. loss functions for optimization attempts on the fitting problem by Adaptive VQKAN for the way 2. (b)(right) Number of epochs vs. sum of absolute distances on the fitting problem by Adaptive VQKAN for the way 2.

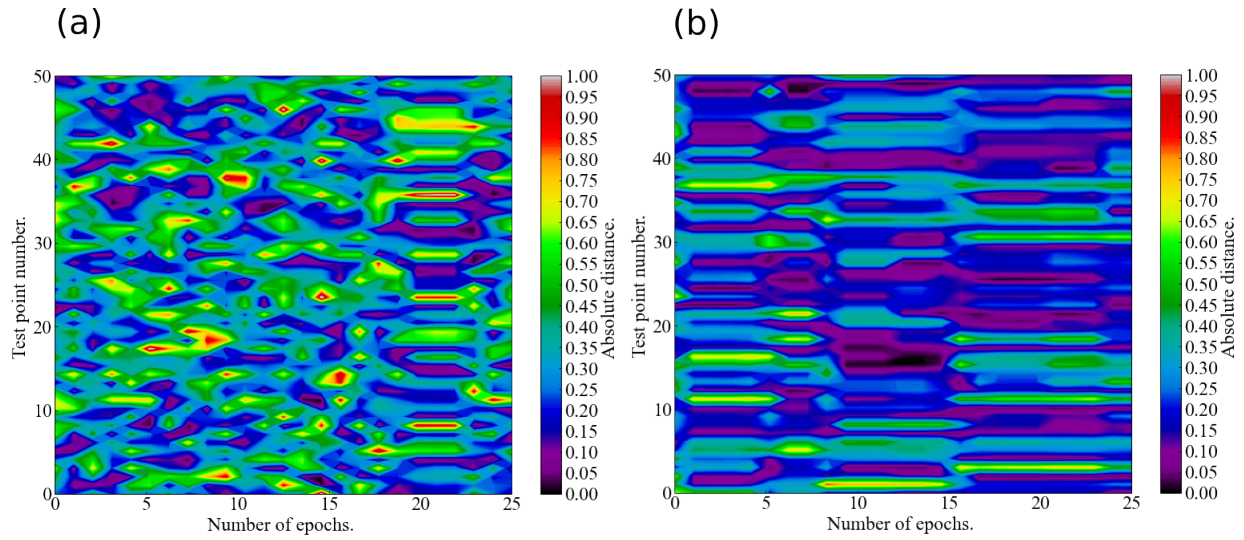
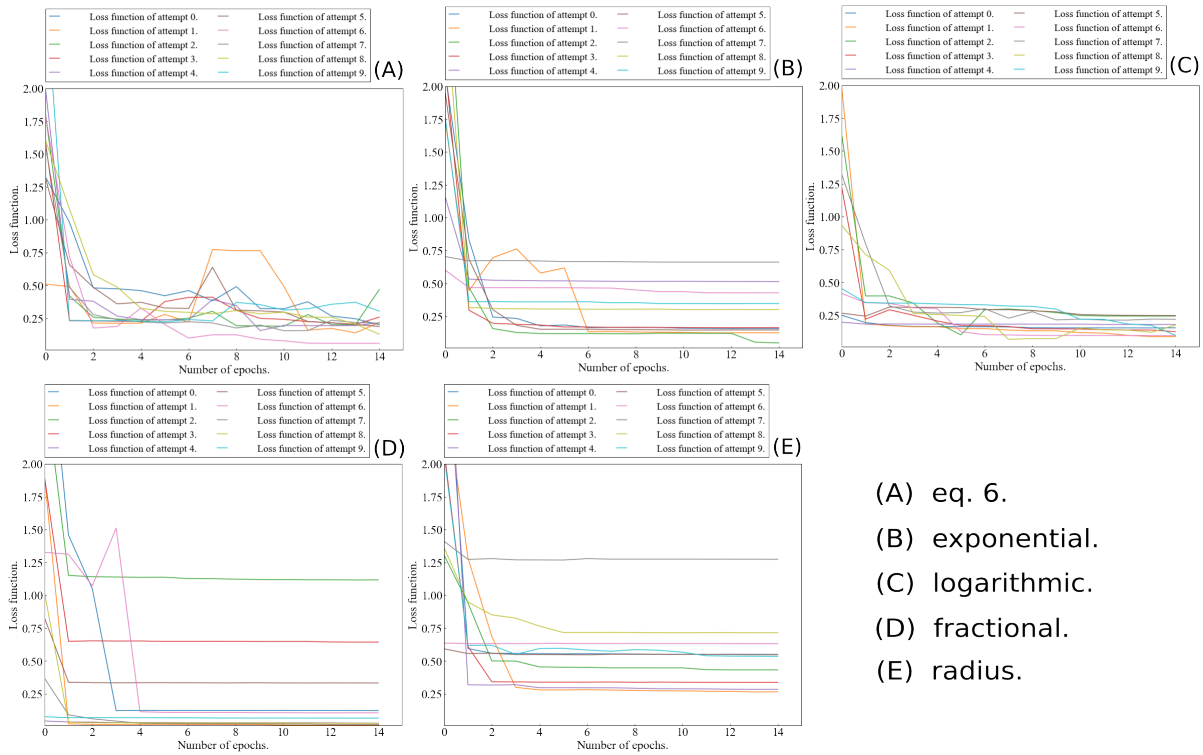


Figure 6. (a) Number of test points and the Number of epochs vs. absolute distances on the fitting problem by Adaptive VQKAN for the way 1. (b) Number of test points and the Number of epochs vs. absolute distances on the fitting problem by Adaptive VQKAN for the way 2.



- (A) eq. 6.
- (B) exponential.
- (C) logarithmic.
- (D) fractional.
- (E) radius.

Figure 7. Number of epochs vs. loss functions for optimization of 10 attempts on the fitting problem of eq. 6, exponential function, logarithmic function, fractional function and radius of sphere by Adaptive VQKAN for the way 2.

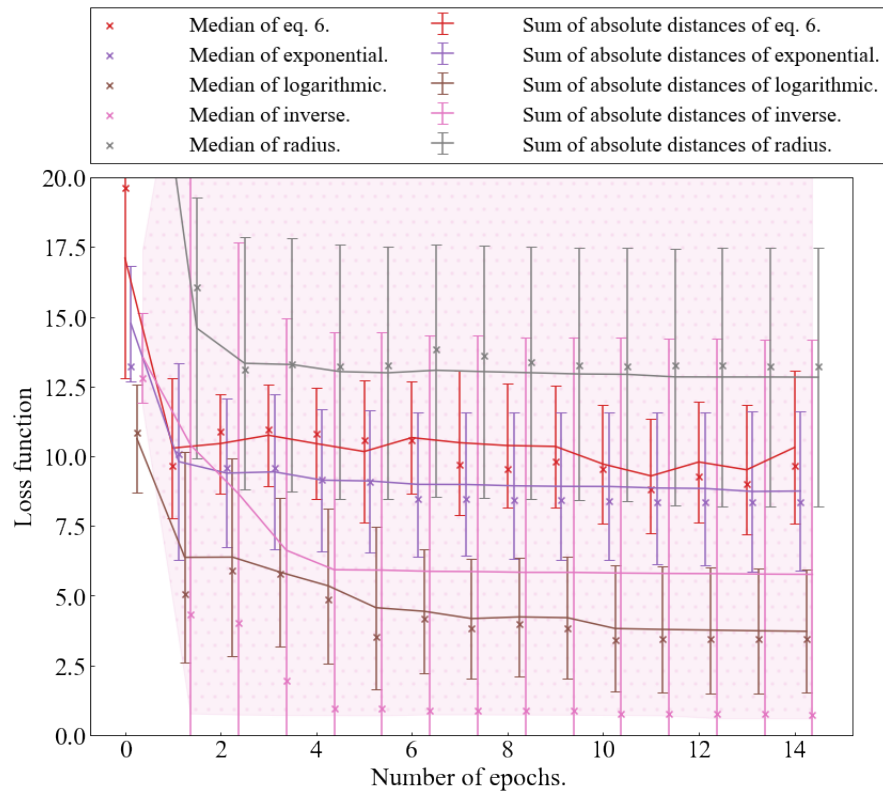


Figure 8. Number of epochs vs. average and median of sum of absolute distances on the fitting problem of eq. 6, exponential function, logarithmic function, fractional function and radius of sphere by Adaptive VQKAN for the way 2. Data of exponential function, logarithmic function, fractional function and radius of sphere are located 0.125 right from before data. The star - hatched area indicates the minimum and maximum values of fractional function.

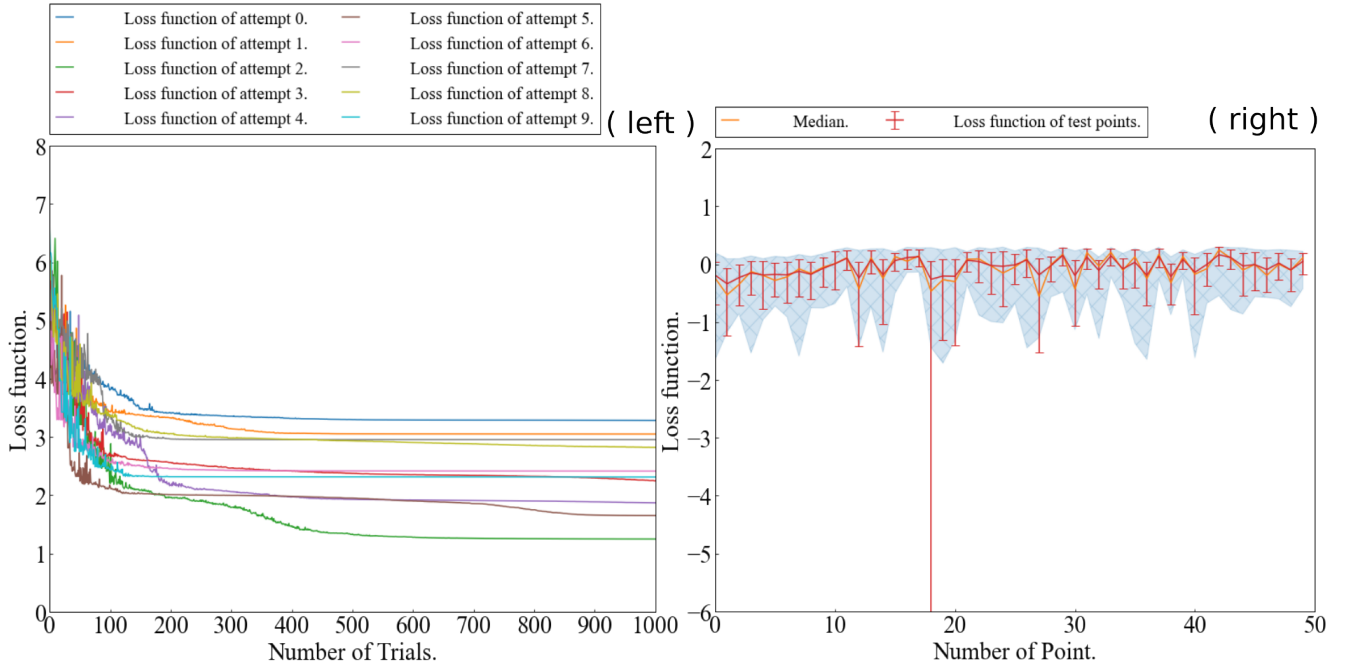


Figure 9. (left) Number of trials vs. loss functions for attempts on optimization using QNN. (right) Number of test points vs. the average and median absolute distances of test points using QNN optimization.

3.2 Classification problem

In this section, we present the results of solving the classification problem for points on a 2-D plane. A point is assigned a label of +1 if it is above the function f and -1 if it is below f . The function f is defined as:

$$f(x) = \exp(d_0x_0 + d_1) + d_2\sqrt{1 - d_3x_0^2} + \cos(d_4x_0 + d_5) + \sin(d_6x_0 + d_7) \quad (7)$$

where d_k represents random coefficients between 0 and 1 for the various cases. The loss function for the classification is given as follows:

$$f^{\text{aim}} = \begin{cases} -1 & \text{if } f \geq x_1 \\ 1 & \text{if } f < x_1 \end{cases} \quad (8)$$

The realm of ${}_n\mathbf{x}^m$ is $\{0, 1\}$. We show the results of the classification for different cases: using QNN with $\dim({}_n\mathbf{x}^m) = 2$ for $n > 2$, using Adaptive VQKAN with $\dim({}_n\mathbf{x}^m) = 2$ for $n > 2$ for single attempt in case the Number of epochs is 25 for the way 2, and using Adaptive VQKAN with $\dim({}_n\mathbf{x}^m) = 2$ for $n > 2$ for 10 attempt with in case the Number of epochs is 15 for the way 2.

In advance, we show the result for QNN. Fig. 9 (left) shows the loss functions for different attempts, while Fig. 9 (right) displays the classification results for 50 randomly sampled points. The calculation has not converged to a global value, and the sum of absolute distances is also large, at an average of 45.902.

Next, We show the value of the loss function, the sum of absolute distance on test points for the Number of epochs, and absolute distances on test points in Figs. 10 (left), 10 (right), 11, respectively for the way 2. The loss function's value hasn't reached the global minimum, but it is larger than the largest attempt of QNN. The sum of absolute distance is also more extensive than those of QNN in all regions of the epoch. In addition, adaptive ansatz never grew. It indicates that non-continuum functions are complex to be optimized by adaptive ansatz.

Next, we show the average of 10 attempts for the value of the loss function and the sum of absolute distance on test points for the Number of epochs in Fig. 12 (left) and 12 (right), respectively, in case the Number of epochs is 15 for the way 2. The value of loss function and the sum of absolute distance are both more significant than all other cases.

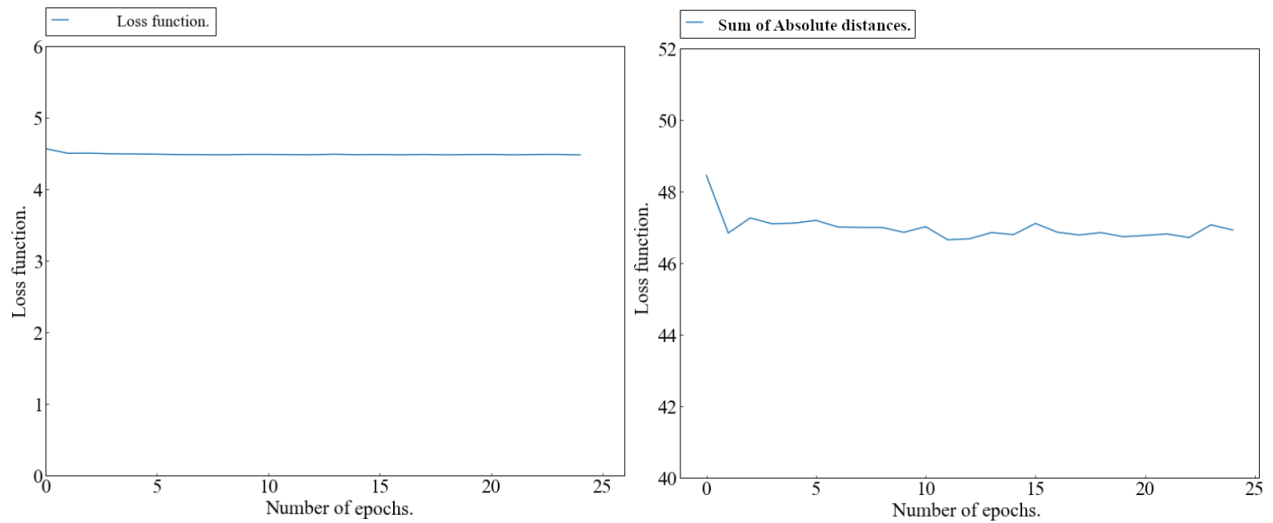


Figure 10. (left) Number of epochs vs. loss functions for optimization attempts on the classification problem by Adaptive VQKAN for the way 2. (right) Number of epochs vs. sum of absolute distances on the classification problem by Adaptive VQKAN for the way 2.

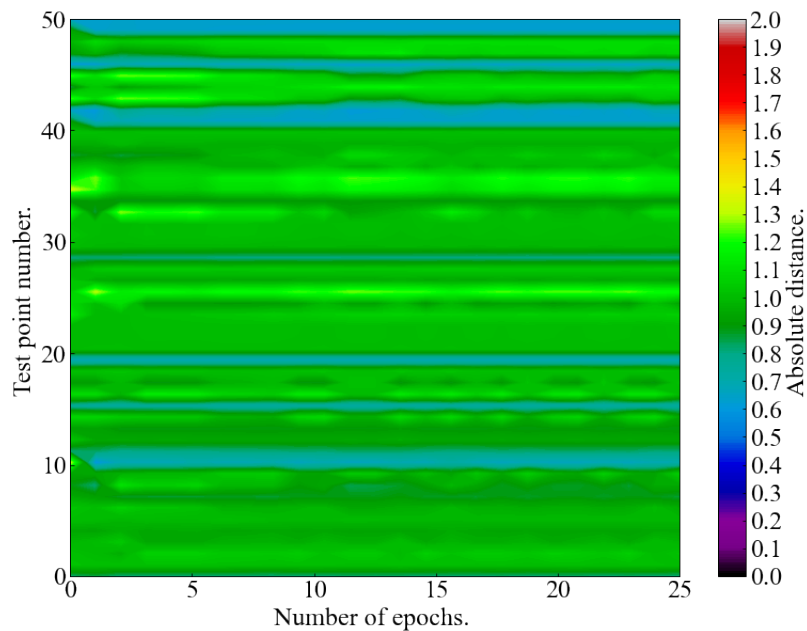


Figure 11. Number of test points and the Number of epochs vs. absolute distances on the classification problem by Adaptive VQKAN for the way 2.

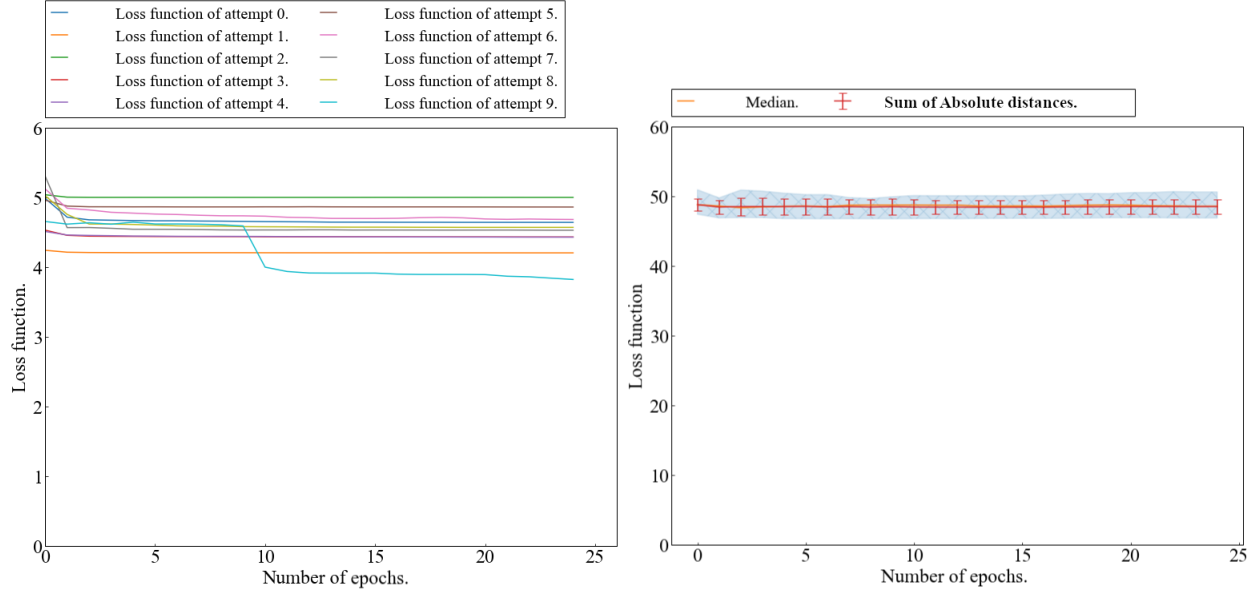


Figure 12. (left) Number of epochs vs. loss functions for optimization of 10 attempts on the classification problem by Adaptive VQKAN for the way 2. (right) Number of epochs vs. average and median of sum of absolute distances on the classification problem by Adaptive VQKAN for the way 2.

3.3 Fourier differential equation

We performed the Adaptive VQKAN on solving a Fourier differential equation of the following equation on 10 sampled points and predicted the values of 50 test points.

The target function is defined as:

$$\frac{\partial u}{\partial t} = \frac{\partial^2 u}{\partial x^2} \quad (9)$$

$$u(0, t) = u(\pi, t) = 0 \text{ border condition.} \quad (10)$$

$$u(x, 0) = \begin{cases} x & 0 \leq x < \frac{\pi}{2} \\ \pi - x & \frac{\pi}{2} \leq x \leq \pi \end{cases} \text{ initial state.} \quad (11)$$

$$u(x, t) = \frac{4}{\pi} \left\{ e^{-t} \sin x - \frac{1}{3^2} e^{-3^2 t} \sin 3x + \frac{1}{5^2} e^{-5^2 t} \sin 5x - \frac{1}{7^2} e^{-7^2 t} \sin 7x + \dots \right\} \quad (12)$$

Here, $u(x, t)$ and $\{x, t\}$ are correspond to f^{aim} and $2_1 \mathbf{x}^m - 1$, ${}_n \mathbf{x}_i^m = 0.5(\langle \tilde{\Psi}({}_1 \mathbf{x}^m) | Z_i | \tilde{\Psi}({}_1 \mathbf{x}^m) \rangle + 1)$ which the realm is normalized in $\{0, 1\}$, with $N_d^n = 2$ and $\dim({}_n \mathbf{x}^m) = 2$ for all layers and calculations, and the Hamiltonian is $Z_0 Z_1 + Z_2 Z_3$. Then, initial state $|\Psi_{\text{ini}}({}_1 \mathbf{x}^m)\rangle$ is $\prod_{j=0}^{N_q-1} R_y^j(2 \text{acos}({}_1 \mathbf{x}^m)) | 0 \rangle^{\otimes N_q}$ for each input m .

The differentiations are processed by the parameter shift rule; the deviation Δx and Δt are 0.0001, and the Number of terms in the aimed function is 10. The differential equation is the conditional term of loss function, hence, the Hamiltonian expectation value is calculated five times for entire loss function, thus, it is conditional fitting problem. The Number of layers $N_l = 1$ and initial ansatz is Z_0 , respectively. In advance, we show the result for QNN. Input on Rx gates are x_i for only this case.

Fig. 13 (left) shows the loss functions for different attempts, while Fig. 13 (right) displays the solving results for 50 randomly sampled points. The value of loss function converged and absolute distances on test points is 6.2873 on average.

Next, we show the value of the loss function, the sum of absolute distance on test points for the Number of epochs, and absolute distances on test points in Figs. 14 (left), 14 (right), 15, respectively for the way 2. The value of the loss function became smaller than that of QNN, though the sum of the absolute distances on test points is more significant than that of QNN. The absolute distance on some test points are nearly 1.0 furthermore those on other points are evenly large.

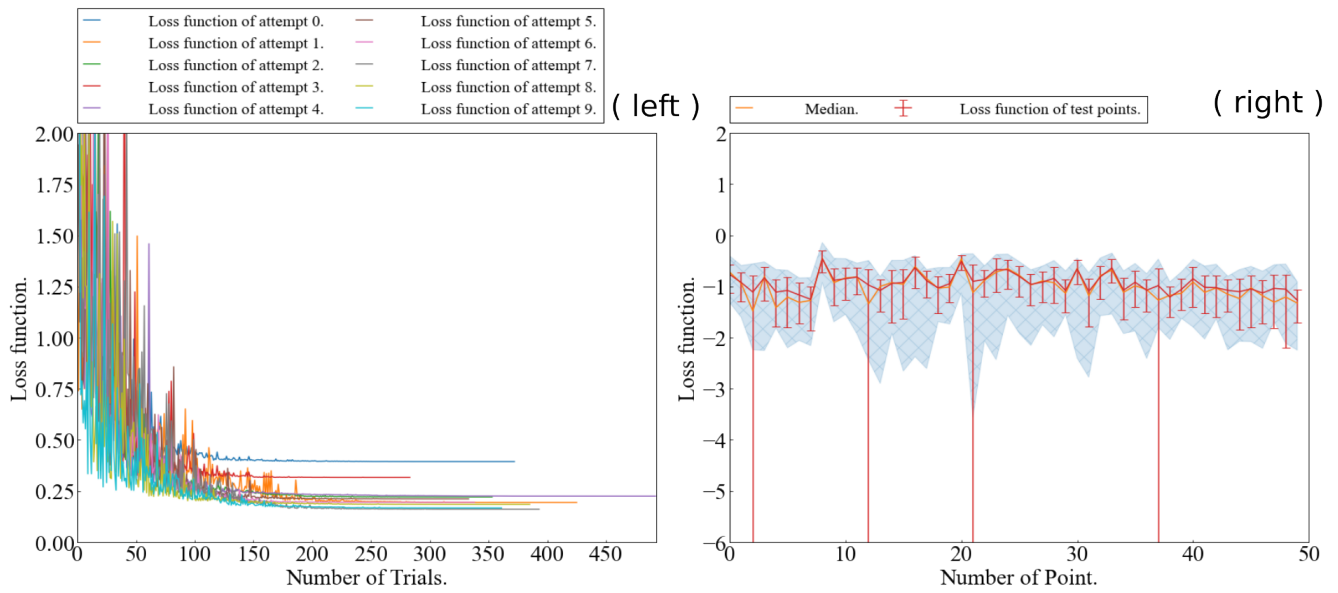


Figure 13. (left) Number of trials vs. loss functions for attempts on optimization using QNN. (right) Number of test points vs. the average and median absolute distances of test points using QNN optimization.

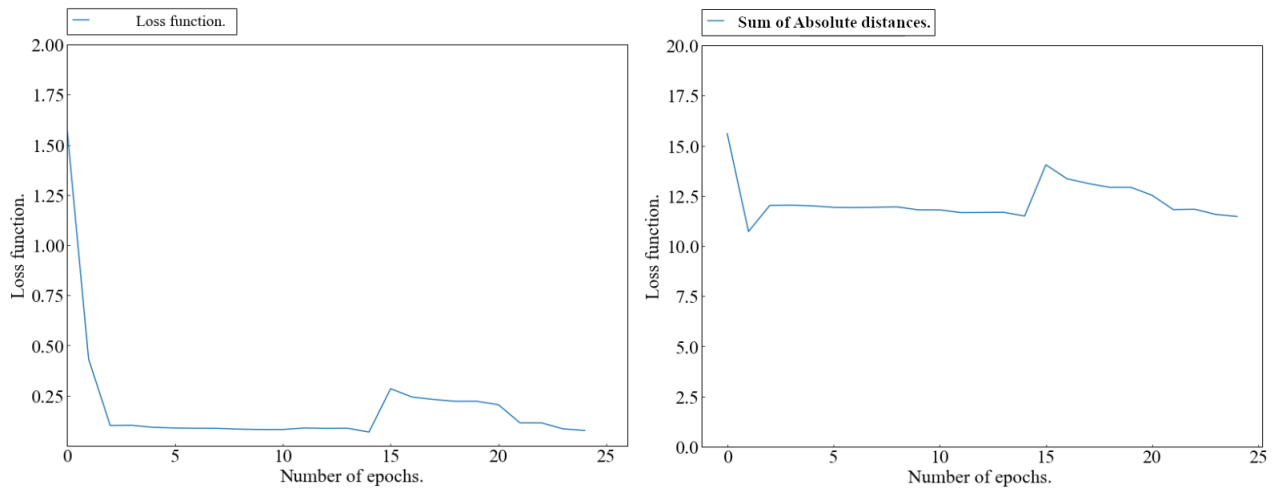


Figure 14. (left) Number of epochs vs. loss functions for optimization attempts on solving a Fourier differential equation by Adaptive VQKAN for the way 2. (right) Number of epochs vs. sum of absolute distances on solving a Fourier differential equation by Adaptive VQKAN for the way 2.

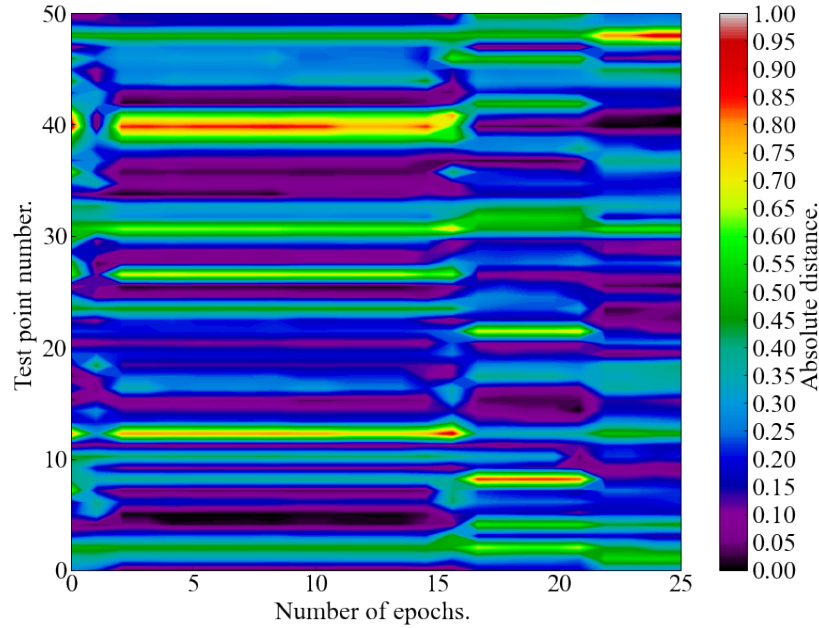


Figure 15. Number of test points and the Number of epochs vs. absolute distances on solving a Fourier differential equation by Adaptive VQKAN for the way 2.

Next, we show the average of 10 attempts for the value of the loss function and the sum of absolute distance on test points for the Number of epochs in Fig. 16 (left) and 16 (right), respectively, in case the Number of epochs is 15 for the way 2.

The values of loss functions are larger than those of except attempt 0 and the minimum sum of the absolute distances is about 6.25, hence, the result of prediction rarely surpasses the average sum of absolute distances on QNN. The accuracy of Adaptive VQKAN is inferior to that of QNN, which is contrary to fitting and classification problems. There are two plausible reasons: we do not use all two-body operators in the operator pool, and the optimization process is cut off before convergence due to a fixed number of trials.

4 Discussion

In this section, we discuss the result of the fitting problem and solving the Fourier differential equation. The operator pool and initial adaptive ansatz are crucial for the accuracy of Adaptive VQKAN. Other reasons for the accuracy are not discussed in this paper. Firstly, we discuss the accuracy of the fitting problem. The accuracy of Adaptive VQKAN is superior to that of QNN on only this problem in this paper. The initial ansatz affects the value of loss functions and the accuracy of prediction as shown in Figs. 17, 18.

We show the values of loss function and the sum of absolute distances on test points of 10 attempts in case (a) initial ansatz is X_0 , (b) initial ansatz is Y_0 , (c) initial ansatz is Z_0 , and (d) initial ansatz is X_0 for two layers, respectively in Figs. 17, 18, respectively. The minimum of the sum of absolute distance is the smallest at epoch 5 in case (a) and the largest at epoch 0 at case (c), respectively. The average of the sum of absolute distances is the smallest at the end of case (c) and the largest in case (b). Even Case (c) has the largest values of loss functions in all, the minimum of the sum of absolute distances is the smallest on average from 1 to 14 for the Number of epochs. The difference among the kinds of initial ansatz is not quite large; however, some kinds of ansatz trap the calculation in overfitting.

The contents of the operator pool may lead to decline of accuracy in some cases as shown in Fig. 19.

From here, operator pool consists of all one and two-body operator.

We show the value of the loss function and the sum of absolute distance on test points for the Number of epochs in Fig. 19 (left) and 19 (right), respectively for the way 1.

The value of loss function fluctuates unstably, however the sum of absolute distances is smaller than that in case the operator pool is limited. Extending the operator pool is effective for the improvement of accuracy on the way 1.

We show the value of the loss function and the sum of absolute distance on test points for the Number of epochs in Fig. 19 (left) and 19 (right), respectively for the way 2.

The value of loss function is larger than that in case the operator pool is limited and the sum of absolute distances is also larger, contrary to the way 1. The operator pool has room for improvement; for example, adding three and four-body operators

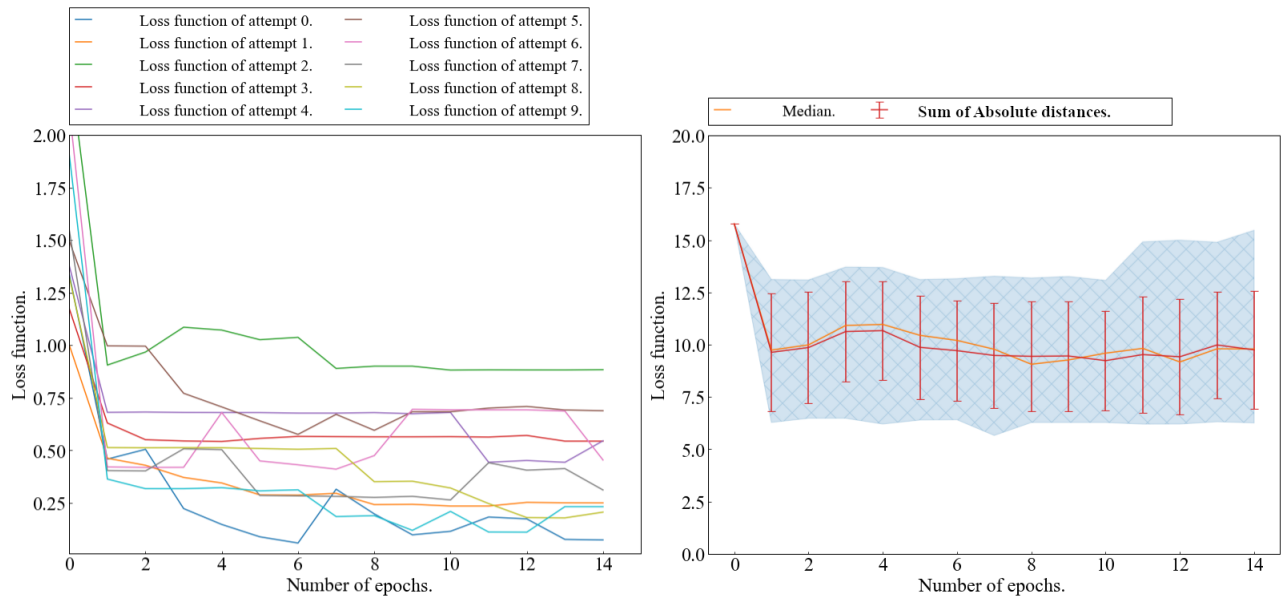


Figure 16. (left) Number of epochs vs. loss functions for optimization of 10 attempts on solving a Fourier differential equation by Adaptive VQKAN for the way 2. (right) Number of epochs vs. average and median of sum of absolute distances on solving a Fourier differential equation by Adaptive VQKAN for the way 2.

or multi-objective optimization that optimizes the contents of the operator pool can also be effective. Secondly, we discuss the result and accuracy of solving the Fourier differential equation. The initial ansatz is effective in the accuracy of solving Fourier differential equations. We show the values of loss function and the sum of absolute distances on test points of 10 attempts in case (a) initial ansatz is Z_0 , and (b) initial ansatz is X_0 for two layers, respectively in Figs. 20, 21, respectively.

Case (b) has smaller values of loss function than case (a) on average, and the sum of the absolute distances in case (b) is larger than case (a) on average too. Solving the Fourier differential equation is only the conditional fitting inside the program; however, effective initial ansatz is different from ordinary fitting.

We show the value of the loss function and the sum of absolute distance on test points for the Number of epochs using the extended operator pool in Fig. 22 (left) and 22 (right), respectively for the way 2.

The value of the loss function is larger than that in case the operator pool is limited; however, the sum of absolute distances is smaller than that in case the operator pool is limited. The QNN is supposed to be good at this problem. Through some techniques, such as modifying the operator pool, the Adaptive VQKAN has the potential to surpass the accuracy of QNN.

The Number of parametric gates is smaller than that of QNN, and the Number of epochs until convergence is only 2; hence, the time for calculation is shorter than that of QNN. The number of parametric gates to converge is at least 2 and 4 at a maximum for succeeded cases on both fitting and solving Fourier differential equation. It is smaller than that of QNN³² and VQKAN¹³, and the time for convergence is as small as that of Filtering VQE³³ which is the fastest VQE^{34,35} in major VQE family.

5 Concluding remarks

In this paper, we revealed that adaptive ansatz contributes to the accuracy of QNN. Besides, required Number of layers and parametric gate are smaller than canonical and compact ansatz to calculate as accurately as them. The Adaptive VQKAN is more accurate than QNN in the fitting problems with respect to both the prediction result and time and in solving differential equations with respect to time. However, this method is not good at optimizing non-continuum functions. The Adaptive VQKAN has room to be improved regarding accuracy and speed. Emulating the function of neurons is possible, for example, propagation of synapses and prospective potential³⁶.

References

1. Yu, Y., Si, X., Hu, C. & Zhang, J. A Review of Recurrent Neural Networks: LSTM Cells and Network Architectures. *Neural Comput.* **31**, 1235–1270, DOI: [10.1162/neco_a_01199](https://doi.org/10.1162/neco_a_01199) (2019). https://direct.mit.edu/neco/article-pdf/31/7/1235/1053200/neco_a_01199.pdf.

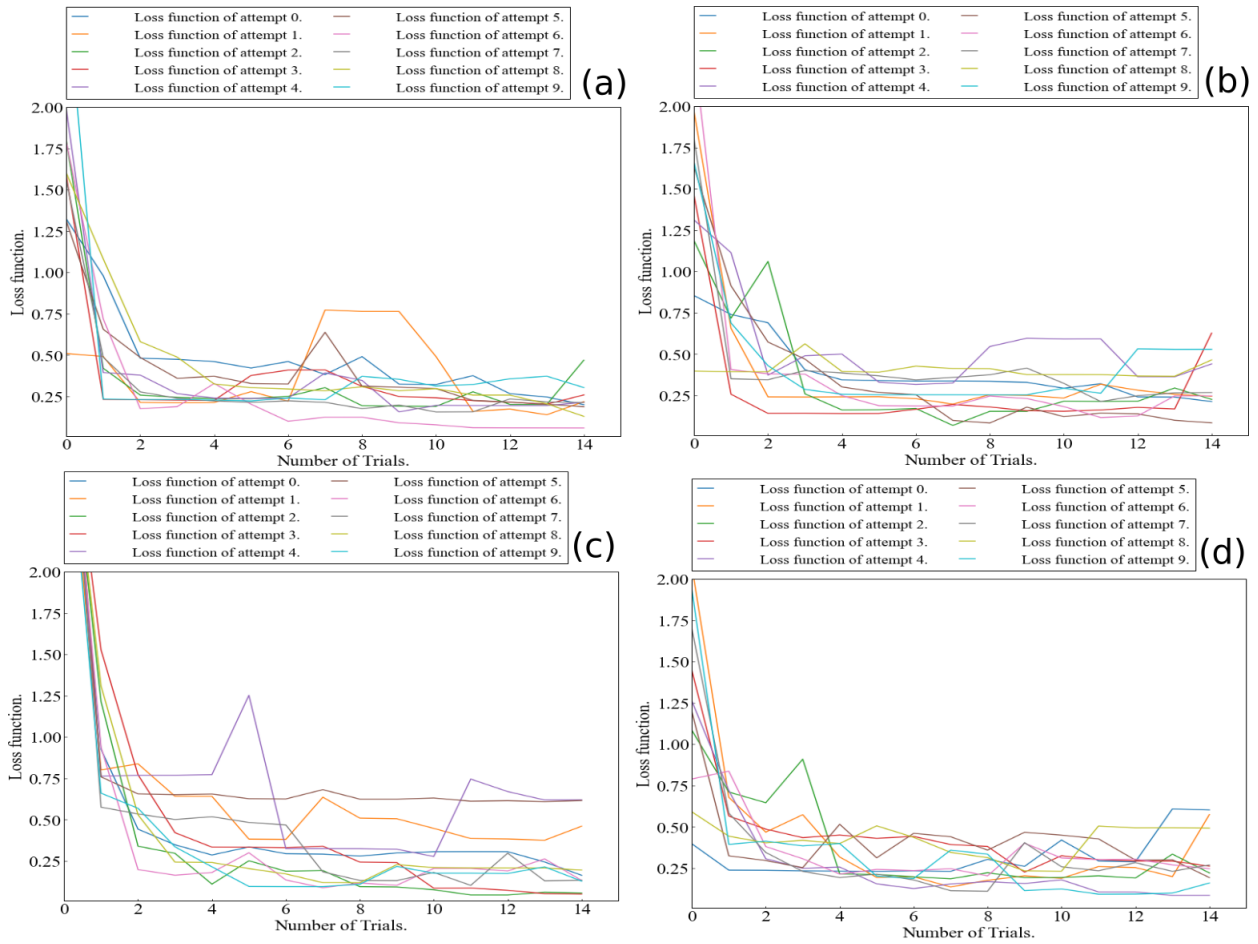


Figure 17. Number of epochs vs. loss functions for optimization of 10 attempts of 10 attempts on the fitting problem in case (a) initial ansatz is X_0 , (b) initial ansatz is Y_0 , (c) initial ansatz is Z_0 , and (d) initial ansatz is X_0 for two layers by Adaptive VQKAN for the way 2.

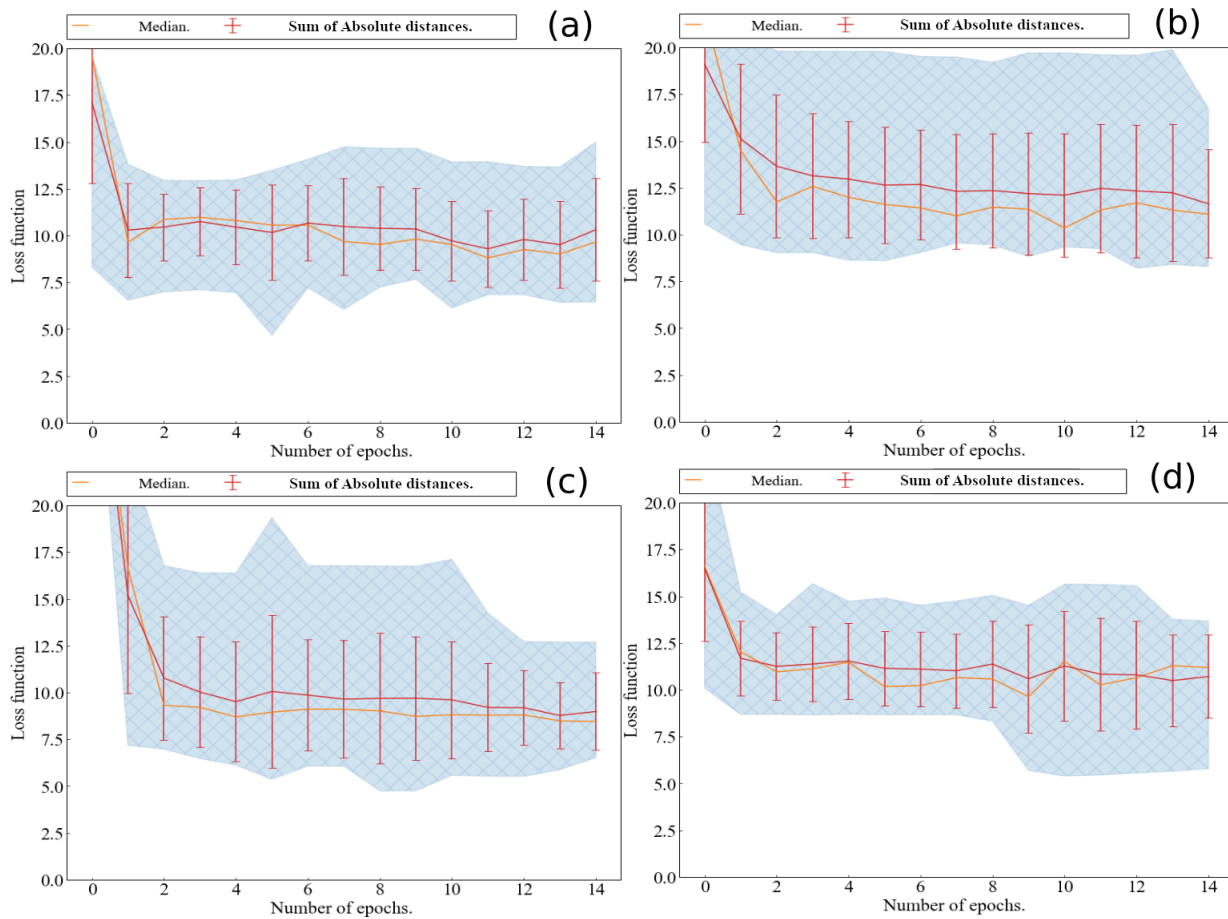


Figure 18. Number of epochs vs. average and median of sum of absolute distances on the fitting problem in case (a) initial ansatz is X_0 , (b) initial ansatz is Y_0 , (c) initial ansatz is Z_0 , and (d) initial ansatz is X_0 for two layers by Adaptive VQKAN for the way 2.

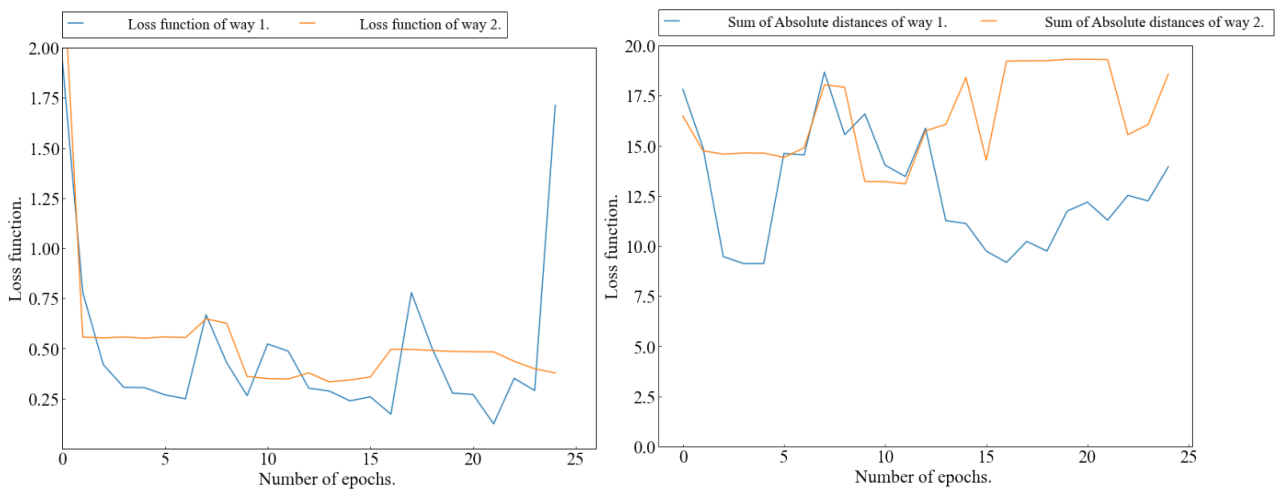


Figure 19. (left) Number of epochs vs. loss functions for optimization attempts on the fitting problem by Adaptive VQKAN using extended operator pool for the way 1 and 2. (right) Number of epochs vs. sum of absolute distances on the fitting problem by Adaptive VQKAN using extended operator pool for the way 1 and 2.

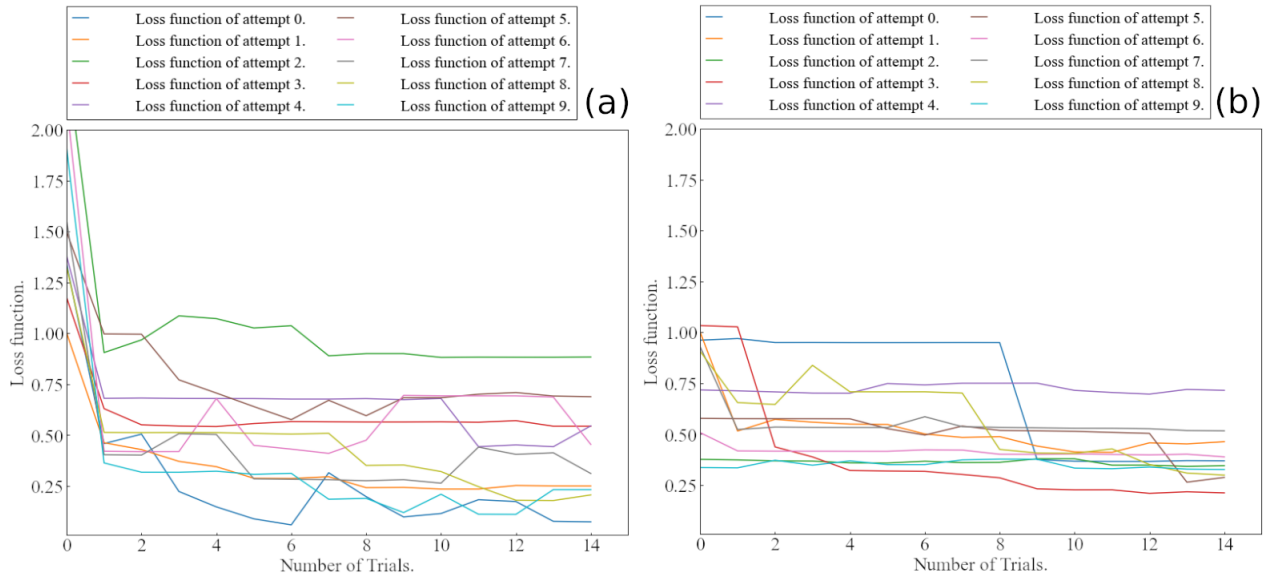


Figure 20. Number of epochs vs. loss functions for optimization of 10 attempts on solving Fourier differential equation in case (a) initial ansatz is X_0 , (b) initial ansatz is Y_0 , (c) initial ansatz is Z_0 , and (d) initial ansatz is X_0 for two layers by Adaptive VQKAN for the way 2.

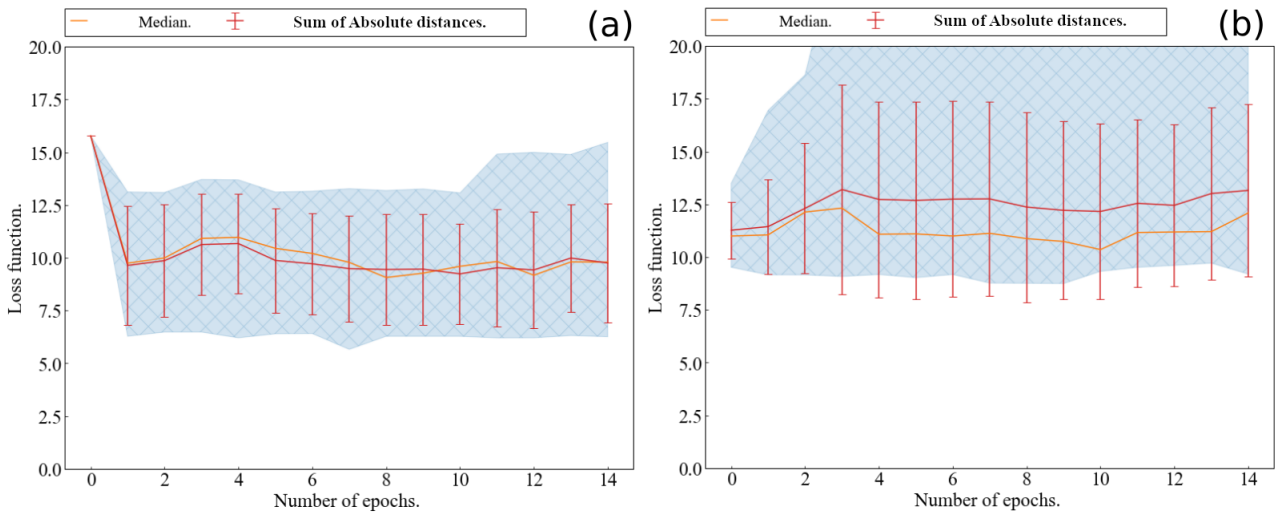


Figure 21. Number of epochs vs. average and median of sum of absolute distances on solving Fourier differential equation in case (a) initial ansatz is X_0 , (b) initial ansatz is Y_0 , (c) initial ansatz is Z_0 , and (d) initial ansatz is X_0 for two layers by Adaptive VQKAN for the way 2.

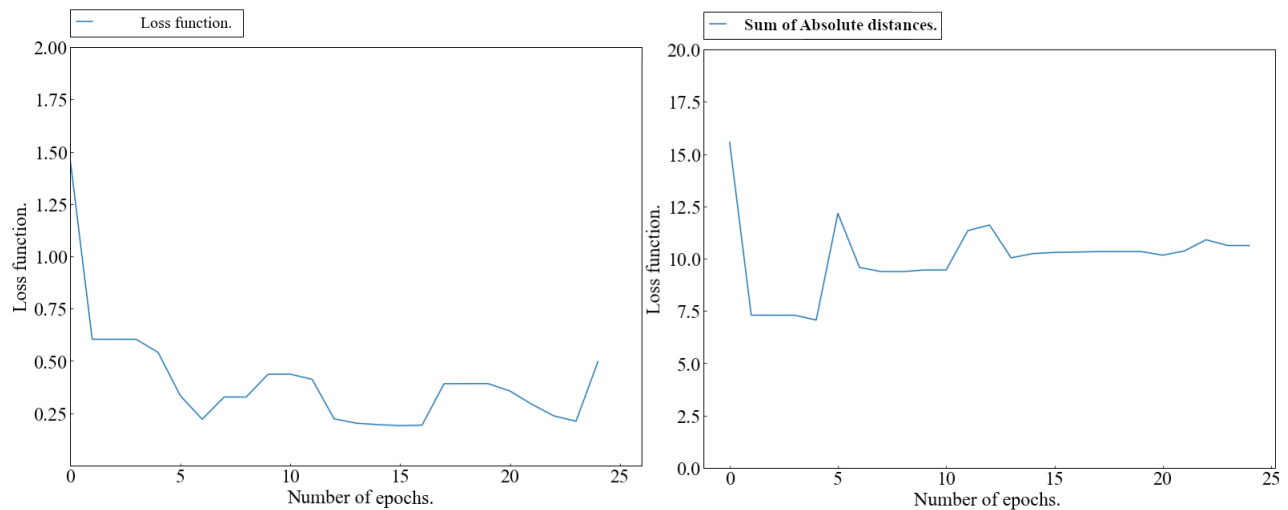


Figure 22. (left) Number of epochs vs. loss functions for optimization attempts on solving a Fourier differential equation by Adaptive VQKAN using extended operator pool for the way 2. (right) Number of epochs vs. sum of absolute distances on solving a Fourier differential equation by Adaptive VQKAN using extended operator pool for the way 2.

2. Masood, A., Naseem, U., Rashid, J., Kim, J. & Razzak, I. Review on enhancing clinical decision support system using machine learning. *CAAI Transactions on Intell. Technol.* **n/a**, DOI: <https://doi.org/10.1049/cit2.12286> (2024). <https://ietresearch.onlinelibrary.wiley.com/doi/pdf/10.1049/cit2.12286>.
3. Xing, Y. & Zhu, J. Deep learning-based action recognition with 3d skeleton: A survey. *CAAI Transactions on Intell. Technol.* **6**, 80–92, DOI: <https://doi.org/10.1049/cit2.12014> (2021). <https://ietresearch.onlinelibrary.wiley.com/doi/pdf/10.1049/cit2.12014>.
4. Ghosh, A., Chakraborty, D. & Law, A. Artificial intelligence in internet of things. *CAAI Transactions on Intell. Technol.* **3**, 208–218, DOI: <https://doi.org/10.1049/trit.2018.1008> (2018). <https://ietresearch.onlinelibrary.wiley.com/doi/pdf/10.1049/trit.2018.1008>.
5. Liu, Z. *et al.* KAN: Kolmogorov-Arnold Networks. *arXiv e-prints* arXiv:2404.19756, DOI: [10.48550/arXiv.2404.19756](https://doi.org/10.48550/arXiv.2404.19756) (2024). [2404.19756](https://arxiv.org/abs/2404.19756).
6. Cang, Y., liu, Y. h. & Shi, L. Can KAN Work? Exploring the Potential of Kolmogorov-Arnold Networks in Computer Vision. *arXiv e-prints* arXiv:2411.06727, DOI: [10.48550/arXiv.2411.06727](https://doi.org/10.48550/arXiv.2411.06727) (2024). [2411.06727](https://arxiv.org/abs/2411.06727).
7. Han, D., Li, Y. & Denzler, J. KAN See Your Face. *arXiv e-prints* arXiv:2411.18165, DOI: [10.48550/arXiv.2411.18165](https://doi.org/10.48550/arXiv.2411.18165) (2024). [2411.18165](https://arxiv.org/abs/2411.18165).
8. Kim, T., Girard, A. & Kolmanovsky, I. CIKAN: Constraint Informed Kolmogorov-Arnold Networks for Autonomous Spacecraft Rendezvous using Time Shift Governor. *arXiv e-prints* arXiv:2412.03710, DOI: [10.48550/arXiv.2412.03710](https://doi.org/10.48550/arXiv.2412.03710) (2024). [2412.03710](https://arxiv.org/abs/2412.03710).
9. Bandyopadhyay, Y., Avlani, H. & Zhuang, H. L. Kolmogorov-Arnold Neural Networks for High-Entropy Alloys Design. *arXiv e-prints* arXiv:2410.08452, DOI: [10.48550/arXiv.2410.08452](https://doi.org/10.48550/arXiv.2410.08452) (2024). [2410.08452](https://arxiv.org/abs/2410.08452).
10. Kou, W. & Chen, X. Machine Learning Insights into Quark-Antiquark Interactions: Probing Field Distributions and String Tension in QCD. *arXiv e-prints* arXiv:2411.14902, DOI: [10.48550/arXiv.2411.14902](https://doi.org/10.48550/arXiv.2411.14902) (2024). [2411.14902](https://arxiv.org/abs/2411.14902).
11. Jahin, M. A., Akmol Masud, M., Mridha, M. F., Aung, Z. & Dey, N. KACQ-DCNN: Uncertainty-Aware Interpretable Kolmogorov-Arnold Classical-Quantum Dual-Channel Neural Network for Heart Disease Detection. *arXiv e-prints* arXiv:2410.07446, DOI: [10.48550/arXiv.2410.07446](https://doi.org/10.48550/arXiv.2410.07446) (2024). [2410.07446](https://arxiv.org/abs/2410.07446).
12. Tang, T., Chen, Y. & Shu, H. 3D U-KAN Implementation for Multi-modal MRI Brain Tumor Segmentation. *arXiv e-prints* arXiv:2408.00273, DOI: [10.48550/arXiv.2408.00273](https://doi.org/10.48550/arXiv.2408.00273) (2024). [2408.00273](https://arxiv.org/abs/2408.00273).
13. Wakaura, H., Bayu Suksmono, A. & Mulyawan, R. Variational quantum kolmogorov-arnold network. *Res. Sq.* DOI: [10.21203/rs.3.rs-4504342/v3](https://doi.org/10.21203/rs.3.rs-4504342/v3) (2024). PREPRINT (Version 3).

14. Kassal, I., Whitfield, J. D., Perdomo-Ortiz, A., Yung, M.-H. & Aspuru-Guzik, A. Simulating chemistry using quantum computers. *Annu. Rev. Phys. Chem.* **62**, 185–207, DOI: [10.1146/annurev-physchem-032210-103512](https://doi.org/10.1146/annurev-physchem-032210-103512) (2011). <https://doi.org/10.1146/annurev-physchem-032210-103512>.
15. McClean, J. R., Romero, J., Babbush, R. & Aspuru-Guzik, A. The theory of variational hybrid quantum-classical algorithms. *New J. Phys.* **18**, 023023, DOI: [10.1088/1367-2630/18/2/023023](https://doi.org/10.1088/1367-2630/18/2/023023) (2016).
16. Grimsley, H. R., Economou, S. E., Barnes, E. & Mayhall, N. J. An adaptive variational algorithm for exact molecular simulations on a quantum computer. *Nat. Commun.* **10**, 3007, DOI: [10.1038/s41467-019-10988-2](https://doi.org/10.1038/s41467-019-10988-2) (2019). [1812.11173](https://doi.org/10.1038/s41467-019-10988-2).
17. Parrish, R. M., Hohenstein, E. G., McMahon, P. L. & Martinez, T. J. Hybrid Quantum/Classical Derivative Theory: Analytical Gradients and Excited-State Dynamics for the Multistate Contracted Variational Quantum Eigensolver. *arXiv e-prints* arXiv:1906.08728 (2019). [1906.08728](https://arxiv.org/abs/1906.08728).
18. Rebstrodt, P., Mohseni, M. & Lloyd, S. Quantum Support Vector Machine for Big Data Classification. *Phys. Rev. Lett.* **113**, 130503, DOI: [10.1103/PhysRevLett.113.130503](https://doi.org/10.1103/PhysRevLett.113.130503) (2014). [1307.0471](https://doi.org/10.1103/PhysRevLett.113.130503).
19. Khoshaman, A. *et al.* Quantum variational autoencoder. *Quantum Sci. Technol.* **4**, 014001, DOI: [10.1088/2058-9565/aada1f](https://doi.org/10.1088/2058-9565/aada1f) (2019). [1802.05779](https://doi.org/10.1088/2058-9565/aada1f).
20. Havlíček, V. *et al.* Supervised learning with quantum-enhanced feature spaces. *Nature* **567**, 209–212, DOI: [10.1038/s41586-019-0980-2](https://doi.org/10.1038/s41586-019-0980-2) (2019). [1804.11326](https://doi.org/10.1038/s41586-019-0980-2).
21. Abel, S., Criado, J. C. & Spannowsky, M. Completely quantum neural networks. *Phys. Rev. A* **106**, 022601, DOI: [10.1103/PhysRevA.106.022601](https://doi.org/10.1103/PhysRevA.106.022601) (2022). [2202.11727](https://doi.org/10.1103/PhysRevA.106.022601).
22. Kwak, Y. *et al.* Quantum Distributed Deep Learning Architectures: Models, Discussions, and Applications. *arXiv e-prints* arXiv:2202.11200 (2022). [2202.11200](https://arxiv.org/abs/2202.11200).
23. Benedetti, M., Coyle, B., Fiorentini, M., Lubasch, M. & Rosenkranz, M. Variational Inference with a Quantum Computer. *Phys. Rev. Appl.* **16**, 044057, DOI: [10.1103/PhysRevApplied.16.044057](https://doi.org/10.1103/PhysRevApplied.16.044057) (2021). [2103.06720](https://doi.org/10.1103/PhysRevApplied.16.044057).
24. Wang, Z. T., Ashida, Y. & Ueda, M. Deep Reinforcement Learning Control of Quantum Cartpoles. *Phys. Rev. Lett.* **125**, 100401, DOI: [10.1103/PhysRevLett.125.100401](https://doi.org/10.1103/PhysRevLett.125.100401) (2020). [1910.09200](https://doi.org/10.1103/PhysRevLett.125.100401).
25. Yang, D., Xiao, Z. & Yu, W. Boosting the Adversarial Transferability of Surrogate Model with Dark Knowledge. *arXiv e-prints* arXiv:2206.08316 (2022). [2206.08316](https://arxiv.org/abs/2206.08316).
26. Mitarai, K., Negoro, M., Kitagawa, M. & Fujii, K. Quantum circuit learning. *Phys. Rev. A* **98**, 032309, DOI: [10.1103/PhysRevA.98.032309](https://doi.org/10.1103/PhysRevA.98.032309) (2018).
27. McClean, J. R., Boixo, S., Smelyanskiy, V. N., Babbush, R. & Neven, H. Barren plateaus in quantum neural network training landscapes. *Nat. Commun.* **9**, 4812, DOI: [10.1038/s41467-018-07090-4](https://doi.org/10.1038/s41467-018-07090-4) (2018).
28. Ivashkov, P., Huang, P.-W., Koor, K., Pira, L. & Rebstrodt, P. QKAN: Quantum Kolmogorov-Arnold Networks. *arXiv e-prints* arXiv:2410.04435, DOI: [10.48550/arXiv.2410.04435](https://doi.org/10.48550/arXiv.2410.04435) (2024). [2410.04435](https://doi.org/10.48550/arXiv.2410.04435).
29. Nakanishi, K. M., Mitarai, K. & Fujii, K. Subspace-search variational quantum eigensolver for excited states. *arXiv e-prints* arXiv:1810.09434 (2018). [1810.09434](https://arxiv.org/abs/1810.09434).
30. Dalton, K. *et al.* Quantifying the effect of gate errors on variational quantum eigensolvers for quantum chemistry. *npj Quantum Inf.* **10**, 18, DOI: [10.1038/s41534-024-00808-x](https://doi.org/10.1038/s41534-024-00808-x) (2024). [2211.04505](https://doi.org/10.1038/s41534-024-00808-x).
31. Kato, T. <https://github.com/Qaqarot>. Opensource software development kit (2018).
32. Wang, L., Sun, Y. & Zhang, X. Quantum transfer learning. *New J. Phys.* **23**, DOI: [10.1088/1367-2630/ac2a5e](https://doi.org/10.1088/1367-2630/ac2a5e) (2021).
33. Amaro, D. *et al.* Filtering variational quantum algorithms for combinatorial optimization. *Quantum Sci. Technol.* **7**, 015021, DOI: [10.1088/2058-9565/ac3e54](https://doi.org/10.1088/2058-9565/ac3e54) (2022). [2106.10055](https://doi.org/10.1088/2058-9565/ac3e54).
34. Sajko, W. J. *Exploring the Potential of the Filtering Variational Quantum Eigensolver*. Master's thesis, Ludwig-Maximilians-Universität München (2023).
35. Marin-Sanchez, G. & Amaro, D. Performance analysis of a filtering variational quantum algorithm. *arXiv e-prints* arXiv:2404.08933, DOI: [10.48550/arXiv.2404.08933](https://doi.org/10.48550/arXiv.2404.08933) (2024). [2404.08933](https://doi.org/10.48550/arXiv.2404.08933).
36. Song, Y. *et al.* Inferring neural activity before plasticity as a foundation for learning beyond backpropagation. *Nat. Neurosci.* **27**, 348–358, DOI: [10.1038/s41593-023-01514-1](https://doi.org/10.1038/s41593-023-01514-1) (2024).